HNPS Advances in Nuclear Physics

Vol 15 (2006)

HNPS2006

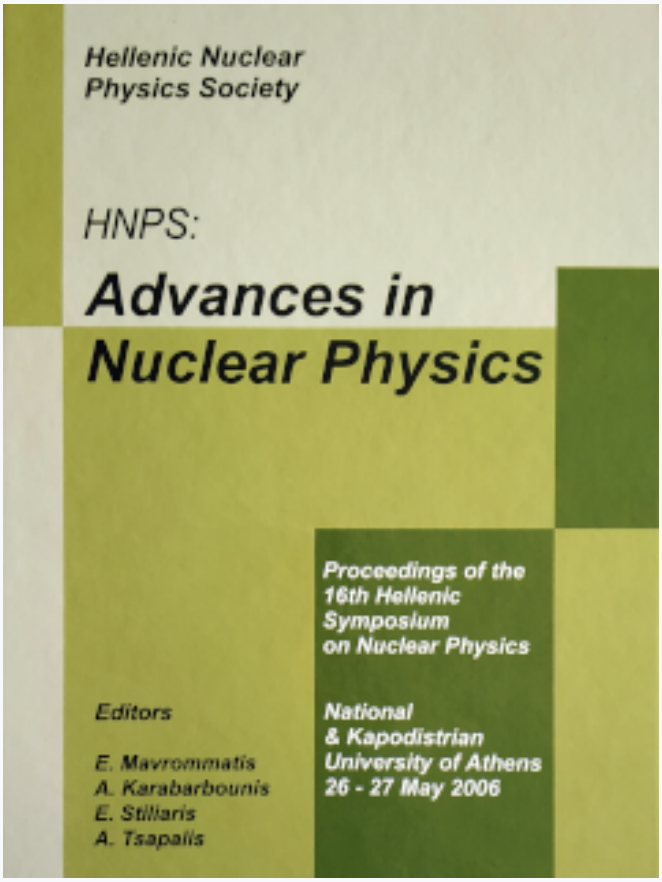


# Sequential binary decay of light nuclear systems: An assessment of statistical model codes

*N. G. Nicolis*

doi: 10.12681/hnps.2623

# Sequential binary decay of light nuclear systems: An assessment of statistical model codes

N.G. Nicolis [a]

[a]Department of Physics, The University of Ioannina, Ioannina 45110,Greece

The sequential decay of excited nuclei is described as a succession of binary processes involving fragments in their ground, excited-bound and unbound states. Primary together with secondary decays lead to the final mass and charge distributions. Asymmetric mass splittings involving nucleon emission up to symmetric binary ones are treated within the Weisskopf evaporation formalism, in a unified manner. This procedure was implemented in the Monte-Carlo multi-step statistical model code MECO (**M**ultisequential **E**vaporation **CO**de). We study the evolution of the calculated final mass and charge distributions from $^{40}$Ar* as a function of the excitation energy, up to complete dissociation. Our results are compared with the predictions of statistical evaporation codes based on different assumptions for the compound nucleus decay.

## 1. INTRODUCTION

Emission of nuclear clusters with A greater than 4 or intermediate mass fragments (IMF) in low and intermediate energy heavy-ion reactions is a topic of current experimental and theoretical interest. IMF emission from equilibrated compound nuclei has been observed in nuclear collisions at energies as low as a few tens of MeV per nucleon. However, several mechanisms may contribute at the same time in the intermediate energy domain. Several models based on different physical assumptions have been developed in order to understand various experimental observables [1,2]. Some of them rely on the concept of mass partition of a thermodynamically equilibrated system in a finite volume, others on a liquid-gas phase transition, cold breakup, percolation concepts or, still, the nuclear disassembly as a sequential decay of an equilibrated compound nucleus, which is the topic of the present work.

In compound nuclei (where the effective fissility parameters are below the Businaro-Gallone point) the saddle- and scission-point configurations are expected to be very close and little damping is expected as the system proceeds between the two [1]. Then, light-particle evaporation and massive binary divisions up to symmetry should be determined by the available phase space at the scission rather than the saddle point configuration. In such cases, a unified description of nucleon evaporation and IMF emission is feasible in the framework of the evaporation formalism.

In the following, we outline the main features of our recently developed extended evaporation model [3] aiming at a unified description of $\gamma$-ray, nucleon, light cluster and IMF emission from an equilibrated compound nucleus. We study the excitation energy

evolution of the final mass and charge distributions in the deexcitation of $^{40}$Ar*. The predictions of our model are compared with the results of other statistical model codes.

## 2. CODE DESCRIPTION AND PARAMETERS

In order to elucidate features of the compound nucleus deexcitation related to sequential binary decay, we developed a Monte-Carlo multistep code involving fragment emission in both ground and excited states (particle-bound or unbound). Gamma-decay, light-particle evaporation and IMF emission are treated in a unified framework, according to the Weisskopf formalism [4].

The decay width $\Gamma(E_0^*, E)$ of emitting a fragment with kinetic energy in the range between $E$ and $dE$ from a compound nucleus with excitation energy $E_0^*$ is

$$\Gamma(E_0^*, E) = \frac{g\mu E\sigma_{inv}(E)}{\pi^2\hbar^2}\frac{\omega(E_f^*)}{\omega(E_0^*)}$$

Here, $\omega(E_0^*)$ and $\omega(E_f^*)$ are the state densities of the compound and the residual nucleus at their respective excitation energies. $\sigma_{inv}(E)$ is the cross section of the inverse process at the center of mass energy E, and g is the spin degeneracy of the emitted fragment.

For fragment emission in unbound states, we employ a generalization of the previous expression to the case when both fragments of a binary division may be excited [5].

$$\Gamma(E_0^*, E) = \frac{\mu E\sigma_{inv}(E)}{\pi^2\hbar^2}\frac{\int_0^{E^*}\omega(\epsilon)\omega(E^*-\epsilon)d\epsilon}{\omega(E_0^*)}$$

Here, $E^*$ is the total available excitation energy of the two fragments.

We assume that gamma decay occurs with dipole E1 transitions. The decay width for gamma emission in the energy range $(\epsilon_\gamma, \epsilon_\gamma + d\epsilon_\gamma)$ is given by

$$\Gamma(\epsilon_\gamma) = \frac{\epsilon_\gamma^2\sigma_\gamma(\epsilon_\gamma)}{(\pi\hbar c)^2}\frac{\omega(E^*-\epsilon_\gamma)}{\omega(E_0^*)}$$

Here, $\sigma_\gamma(\epsilon_\gamma)$ is the inverse (absorption of $\gamma$) cross section assumed to have a Lorentzian energy-dependence with parameters given in Ref. [8].

Pairing corrected state densities are calculated according to the Fermi gas model. Inverse cross sections for light particles and heavy fragments are calculated with the optical model with parameters extrapolated from the compilation of Ref. [6], in accordance with Ref. [7].

The Monte-Carlo procedure was implemented in the code **MECO** (**M**ulti-sequential **E**vaporation **CO**de) [3]. Binary mass divisions of the decaying compound nucleus up to symmetry are considered, taking into account the excitation energy division (according to the available phase space) among the available bound, excited-bound and unbound states of the two fragments. Decays of the secondary fragments are described within the same framework, by feeding the events of the primary emitted unbound fragments into MECO. Their deexcitation was calculated and the event structure was updated, in order to preserve correlations with the primary decay sequence. Stable primary species together with the products of secondary decays lead to the final mass and charge distributions.

Statistical model calculations were performed for the deexcitation of $^{40}$Ar* at five initial excitation energies, corresponding to 1.1, 2.5, 4.5, 7.0 and 10.1 $MeV/A$. In each case, a compound nucleus cross section of 1 barn was assumed. A total of 179 decay channels were considered. They consisted of $\gamma$, n and the ground states of $^{1-3}$H, $^{3-5}$He, $^{6-8}$Li, $^{7-9}$Be, $^{8-12}$B, $^{10-16}$C, $^{12-18}$N, $^{15-21}$O, and $^{16-20}$F, covering the range from extreme asymmetric up to symmetric divisions. A total of 111 excited bound states were included for Li and heavier fragments. Unbound excited states were considered for B and all heavier fragments; a total of 22 isotopes. A nuclear level density parameter $a = A/8.0\,MeV^{-1}$ was assumed.

Figure 1 shows the calculated mass distributions in the deexcitation of $^{40}$Ar* at the five initial excitation energies. Shaded histograms represent the masses of evaporation residues, light emitted particles and IMFs in their ground states. With increasing excitation energy, the evaporation residue mass peaks become broader and shift down in mass. The hatched histograms show the distributions of IMFs emitted in particle-bound excited states. They involve masses $A \approx 5 - 10$ at all excitation energies. IMFs emitted in particle-unbound states are shown with solid histograms. Note that these masses vary from A=10 up to A=20, corresponding to symmetric fission of the compound nucleus. The deexcitation process is completed by allowing the unbound species to decay.

## 3. MODEL COMPARISONS

We have compared the MECO predictions for the final mass (and associated charge) distributions with the results of the statistical model codes PACE [9], SOS [10], and GEMINI [11]. Briefly, the main characteristics of these codes are as follows:

- In the statistical model code PACE, the compound nucleus is assumed to decay by n, p, $\alpha$, $\gamma$ and symmetric fission. Decay probabilities are calculated with the Hauser-Feshbach expression, using Fermi-gas level densities and optical model transmission coefficients. Angular momentum coupling between the initial and final state in the continuum is considered.

- In the code SOS, both evaporation and sequential binary division are treated consistently within the framework of the canonical transition stage theory. Excitation energy division between the two massive fragments of a binary decay is made in proportion to each fragment's mass (i.e. with a constant temperature assumption). Level densities are calculated with a simple exponential function.

- In GEMINI, a hybrid treatment is employed. IMF emissions are calculated with the transition stage theory. The excitation energy division between two massive fragments is made in proportion to each fragment's mass. The Hauser-Feshbach formalism is used for nucleon and light cluster emission, using Fermi-gas level densities and ingoing-wave boundary condition transmission coefficients [12].

Calculations with PACE and GEMINI were performed at zero initial spin. This choice produces some consistency, in the beginning of the deexcitation, with the results expected by the Weisskopf approximation. However, it does not exclude the possibility of angular

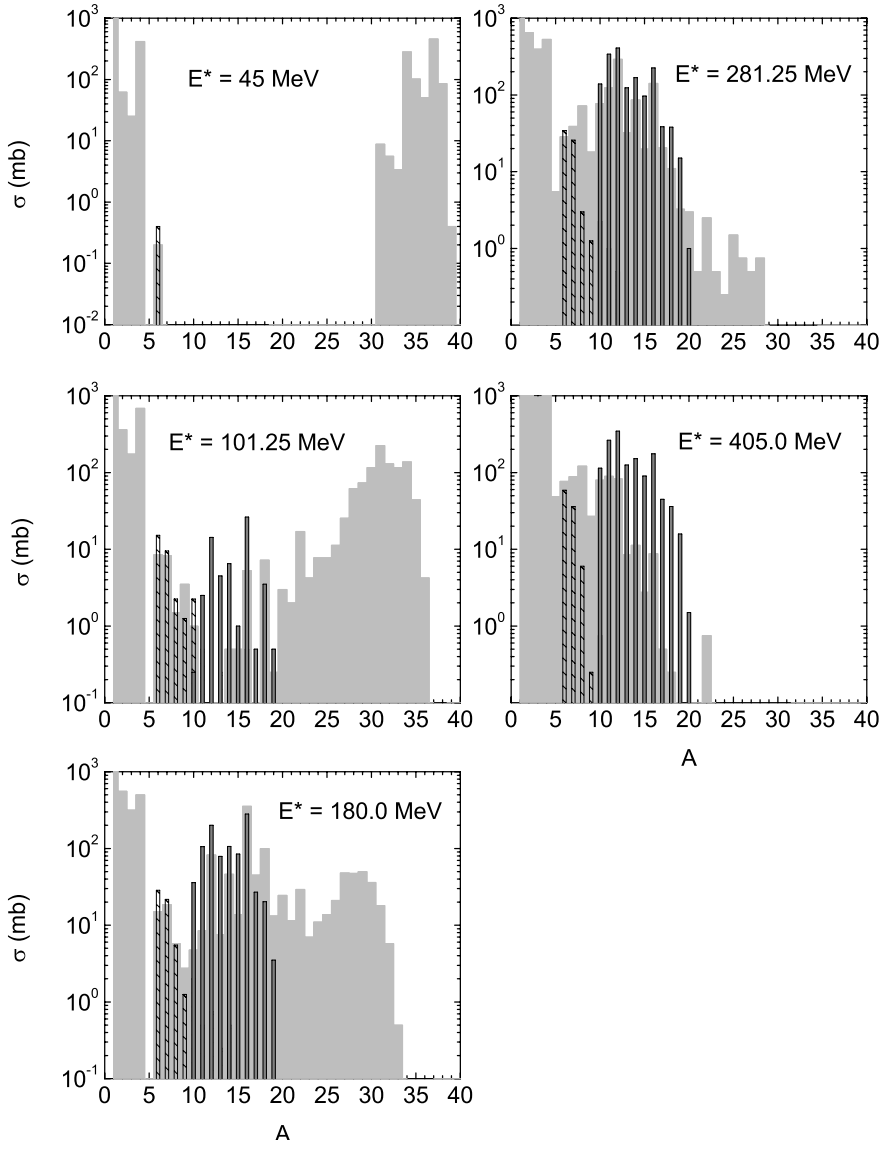


Figure 1. Mass distributions in the statistical decay of $^{40}$Ar* at the indicated initial excitation energies, calculated with MECO. Primary cooled-down residue masses plus emitted fragments, IMF's in excited bound and unbound states are shown with shaded, hatched and solid histograms, respectively.

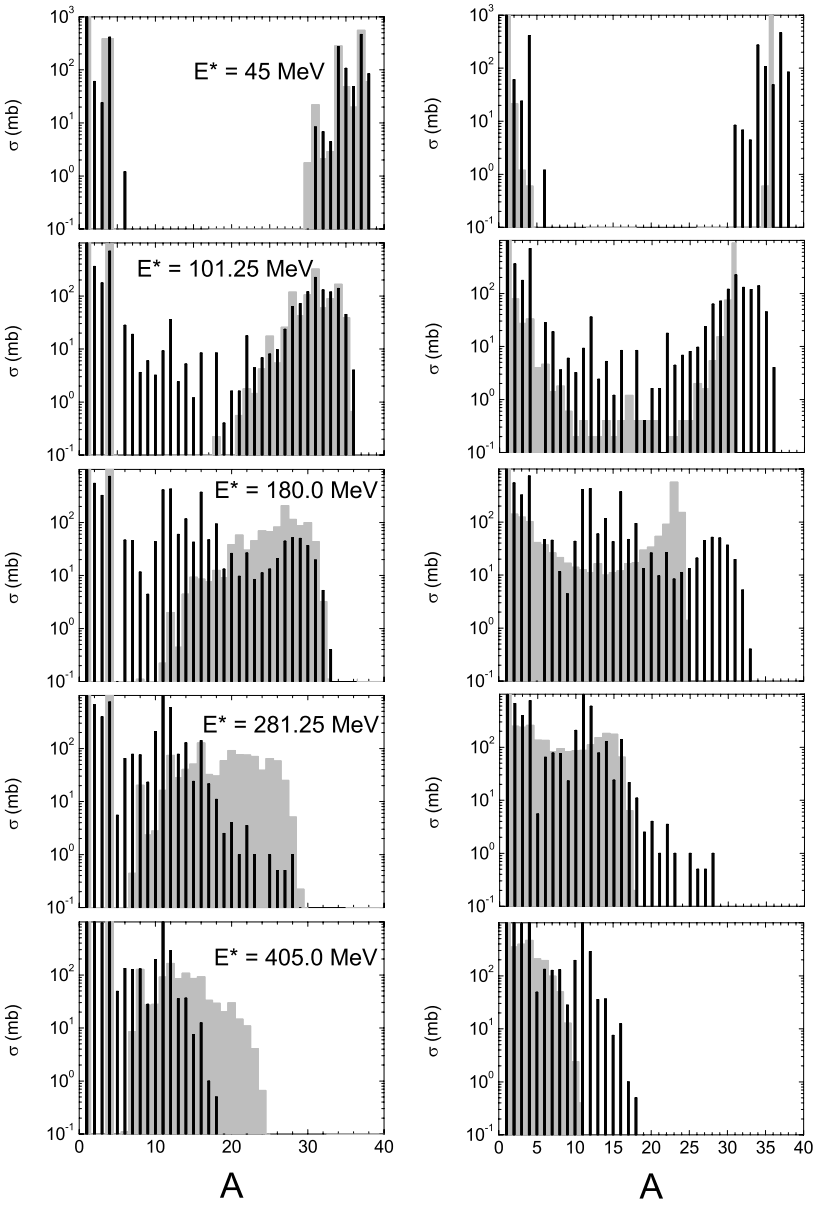


Figure 2. Final mass distributions from the statistical decay of $^{40}$Ar*, at the indicated initial excitation energies. In both panels, calculations with MECO are shown with the solid histograms. Shaded histograms refer to calculations performed with the codes PACE (left) and SOS (right panel).

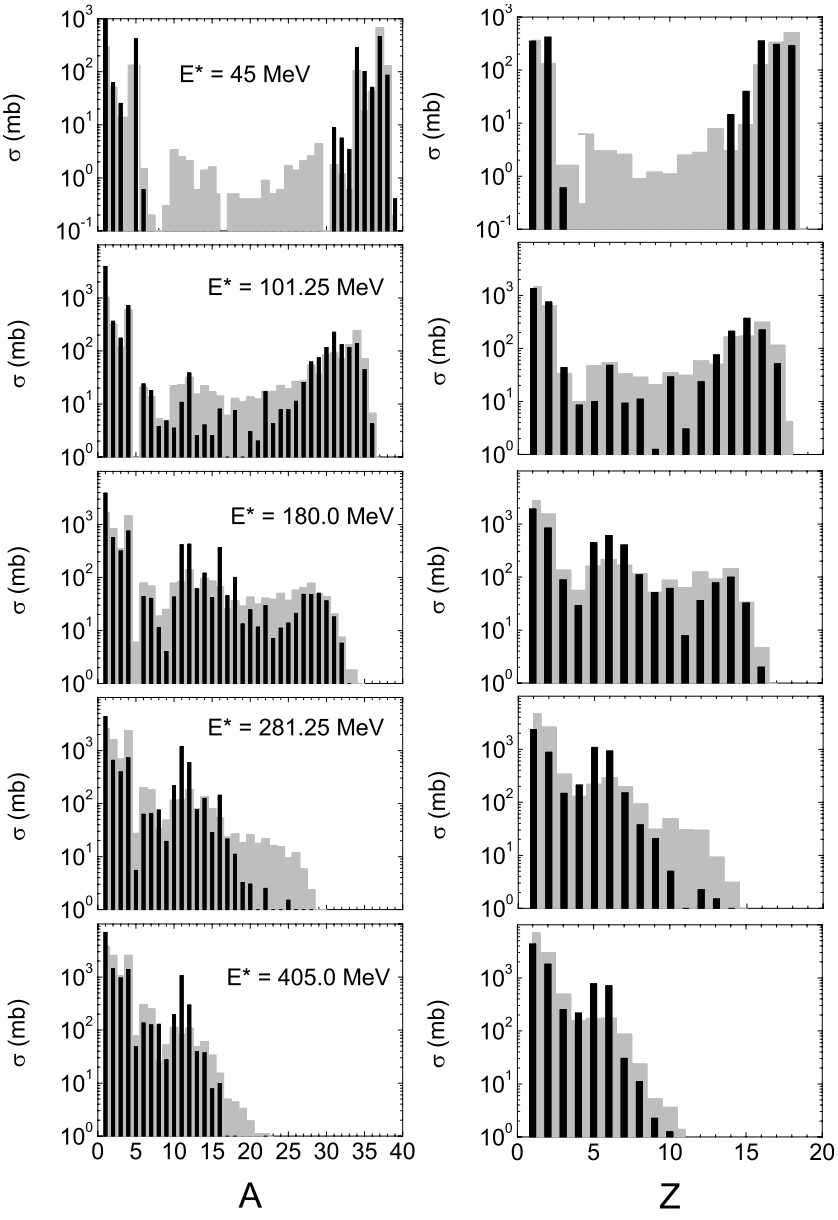


Figure 3. Final mass and charge distributions from the statistical decay of $^{40}$Ar*, at the indicated initial excitation energies. Calculations with MECO and GEMINI are shown with solid and shaded histograms, respectively.

momentum changing transitions during the intermediate decay steps. In all cases, the level density parameter was set equal to $a = A/8.0\,MeV^{-1}$.

The final mass distributions calculated with MECO and PACE are compared on the left column of Figure 2. The two codes produce very similar evaporation residue distributions at the lowest excitation energies, where n, p, $\alpha$ and $\gamma$ emission dominates. However, already at E*=101.25MeV, MECO predicts a significant IMF emission. At the two highest excitation energies, the MECO evaporation residue mass distribution appears shifted down in mass by a greater amount than PACE, because it allows for the emission of additional and more massive decay channels. The amount of symmetric fission predicted with PACE was found negligible. The consistency of the two codes at the lowest excitation energies is encouraging for the predictive power of MECO, since PACE has been able to reproduce a large body of experimental low-energy data from fusion-evaporation reactions. Yet, the MECO predictions for IMF emission remain to be confronted with the experiment.

The comparison between the MECO and SOS mass distributions is shown on the right column of Fig. 2. At low E*, the code SOS predicts a very narrow E.R. mass distribution. Then, a broad U-shaped distribution appears. It becomes more narrow with increasing E* and ends up in a single peaked low-A distribution. In general, we realize strong deviations in the predictions of the two codes at low E* and some tendancy to produce similar results at the highest excitation energies.

Figure 3 shows the mass and charge distributions calculated with MECO and GEMINI. At E*=180.0 MeV, the two codes produce similar results in mass and charge. However, GEMINI produces some excess of IMF production at the lowest excitation energies and some persistence of the heaviest residues at the highest excitation energies. Compared with the previous codes, GEMINI shows a better overall agreement with the MECO results.

## 4. SUMMARY

Concluding, we outlined the basic features of the Monte-Carlo multi-sequential binary decay statistical model code MECO. We studied the evolution of the calculated mass and charge distributions in the deexcitation of the compound nucleus $^{40}$Ar*, in a wide range of excitation energies. Comparisons were made with the predictions of other statistical model codes. The comparison with PACE shows a consistency with MECO at low excitation energies. Differences observed at higher excitation energies are due to the enhanced phase space allowed in MECO. Large differences are observed with the predictions of the code SOS. However, these differences become smaller at highest excitation energy, where binary decay competes strongly with nucleon emission. Regarding the GEMINI code, we observe a reasonable agreement at all excitation energies. Differences between the two codes, such as the low energy thresholds for IMF emission predicted by GEMINI, deserve an investigation through comparisons with experimental data.

## REFERENCES

1. L.G. Moretto and G.J. Wosniak, Prog. Part. Nucl. Phys. **21**, 401(1988).
2. D.H.E. Gross, Rep. Prog. Phys. **53** 605(1990).

3. N.G. Nicolis, *Proceedings of the 15th Symposium of the Hellenic Nuclear Physics Society*, Aristotle University of Thessaloniki, Thessaloniki, Greece, May 27-28, 2005.
4. V. Weisskopf, Phys. Rev. **52**, 295(1937); Phys. Rev. **57**, 472(1940).
5. M.A. Preston, Physics of the Nucleus, Reading Massachussetts, Palo Alto. London: Addison-Wesley Publishing Company (1962).
6. C.M. Perey and F.G. Perey, At. Nucl. Data Tables **17**, 1(1976).
7. J. Gomez del Campo *et al.*, Phys. Rev. C**43**, 2689(1991).
8. A.S. Iljinov *et al.*, Nucl. Phys. A**543**, 517(1992).
9. A. Gravron, Phys. Rev. C**21**, 230(1980).
10. J.A. López and J. Rundrup, Nucl. Phys. A**491**, 477(1989).
11. R.J. Charity *et al.*, Nucl. Phys. A**483**, 317(1988).
12. J.M. Alexander, M.T. Magda and S. Landowne, Phys. Rev. C**42**, 1092(1990).